JOURNAL OF GUIDANCE, CONTROL, AND DYNAMICS
Vol. 21, No. 3, May–June 1998

Tactical Missile Guidance with Passive Seekers Under High Off-Boresight Launch Conditions

Paul L. Vergez*
U.S. Air Force Academy, Colorado Springs, Colorado 80840-6224

For future short-range air-to-air missile concepts, it has been recently demonstrated that throttleable hybrid rocket motors, coupled with linear optimal guidance laws, provide significant performance improvements over traditional solid rocket motors utilizing similar guidance laws in high off-boresight launch conditions. A problem associated with these optimal guidance laws is that they require missile-to-target position, velocity, and acceleration. For practical missile applications, only the initial values of relative position and velocity and an initial guess of the target's acceleration would be available from the launching aircraft. To further complicate the situation, most short-range missiles use a passive seeker, providing angle-only measurements, and accelerometers to measure the missile's accelerations. An extended Kalman filter (EKF) is developed to estimate the required guidance information using passive seeker measurements. The performance of a missile with a passive seeker in high off-boresight launch conditions is evaluated using the combination of an EKF and the guidance law. In particular, a comparison is made between three guidance schemes using estimated states from an EKF. The three guidance schemes are 1) an optimal guidance law coupled with a solid rocket motor, 2) an optimal guidance law coupled with a hybrid rocket motor, and 3) proportional navigation coupled with a solid rocket motor. The results show that the optimal guidance law coupled with a hybrid rocket motor provides a significant improvement in high off-boresight, air-to-air engagements over proportional navigation and the optimal guidance law coupled with a solid rocket motor.

Introduction

THERE has been a renewed interest in expanding the launch envelope of short-range air-to-air tactical missiles.[1,2] Since the late 1970s, the application of optimal control theory to the missile guidance problem has been extensively evaluated.[3–5] For the current Sidewinder-type missile, guidance laws developed from linear quadratic Gaussian (LQG) theory have provided significant performance improvements over the more conventional proportional navigation guidance law.[6] These performance evaluations have been limited to launch situations where the target is within 40-deg off-boresight (angle between the nose of the missile and the target).[4] This was primarily due to the limited maneuver capability of the missile. Research advances in missile airframe design and thrust vectoring have demonstrated that the launch envelope can be expanded to high off-boresight launch conditions (40–90 deg).[1,2] These technologies improve the maneuverability of the missile, thus enabling the missile to pull sharp turns in the direction of the target.

Another technology that deserves attention is hybrid rocket motors. These motors are like the traditional solid motors in that they have a solid fuel core; however, the oxidizer (usually a gas or liquid) is kept in a separate chamber. By controlling the flow of the oxidizer, the rocket motor can be throttled. In a high off-boresight launch condition, the missile could reduce its thrust, pull a sharp turn to point at (or lead) the target, and then increase thrust to intercept. The issue then is how to smartly control the thrust of the missile under varying launch conditions.

An advanced guidance law has been developed from LQG theory for a Sidewinder-type missile using a hybrid rocket motor.[7] The advanced guidance law provides both pitch and yaw acceleration commands as well as an axial thrust command to the hybrid motor. This guidance law, coupled with a hybrid rocket motor, has shown significant improvements in launch envelopes for high off-boresight launch conditions when compared with optimal guidance laws using traditional solid rocket motors. A significant advantage of this guidance law/hybrid rocket motor combination is that it can be adapted to current Sidewinder missiles, thus improving the performance of existing missiles. A critical assumption used to develop these guidance laws is that the missile-to-target position, velocity, and acceleration are known. This is not true given today's tactical missiles. In many cases, passive seekers are used to provide a measure of line-of-sight angle and angle rate. In addition, the missile's accelerations are known through onboard accelerometers.

A widely accepted theory used to estimate the necessary relative position, velocity, and acceleration is Kalman filtering. Much work has been done applying this theory to the tactical missile guidance problem, in particular, the use of extended Kalman filters (EKFs).[4]

The purpose of this research is to investigate the use of an EKF to estimate the necessary information for the advanced guidance law coupled with a hybrid rocket motor in high off-boresight launch conditions, given passive seeker information and the missile's accelerations. The performance of this guidance package will be compared with a similar advanced guidance law coupled with a solid rocket motor and proportional navigation coupled with a solid rocket motor. A brief discussion of hybrid rocket motors is presented first.

Hybrid Rocket Motors

All current tactical air-to-air missiles are fueled by solid propellant rockets motors. These motors consist of a mixture of fuel and oxidizer blended together and solidified.[8] The advantages of solid rocket motors are that they are simple and can be stored for long periods of time before use. The main disadvantage is that once they are ignited, they cannot be shut off. They will burn until the fuel is spent. The thrust profile can be controlled, to some extent, by shaping the fuel core of the solid motor to adjust the surface area.[8] This is done in the factory and cannot be modified in flight. For a short-range air-to-air tactical missile, the vehicle will pull most of its acceleration in the first 2–5 s. At that point, the missile has a significant speed advantage over its target and has to rely on aerodynamic maneuvering to hit the target. The problem comes up in a short-range engagement where the target is in a high off-boresight position. Because the missile is pulling virtually maximum acceleration in its axial direction for the first several seconds, it is limited in its ability to pull lateral accelerations to intercept the target. If the missile could throttle its motor, it could slow its axial acceleration to allow for increased lateral acceleration. Liquid rocket engines have the advantage of throttling; however, they cannot achieve the same thrust levels as solid motors, and they are more complex to operate and therefore more prone to failure.

Received May 22, 1997; revision received Nov. 9, 1997; accepted for publication Nov. 9, 1997.

*Lt. Col., Associate Professor of Astronautics, Department of Astronautics, 2354 Fairchild Drive, Suite 6J75.

Hybrid rocket engines combine the best characteristics of the solid rocket systems and the liquid rocket systems. In a hybrid rocket, the fuel (which is usually a solid) is kept separate from the oxidizer (usually a liquid or gas). The process involves injecting the oxidizer into a thrust chamber lined with the solid fuel. Once ignited, the oxidizer combines with the fuel and burns. By adjusting the flow rate of the oxidizer, the engine can be throttled. Since the late 1980s, there has been much research in developing and improving these rocket motors.[7] This technology has matured to the point that hybrid rocket motors are ready for development. The U.S. Air Force Academy launched a 6.1-m sounding rocket using a hybrid rocket motor in 1994, which flew to an altitude of 4600 m.

The primary advantages of a hybrid rocket engine are 1) throttleability (just mentioned), 2) higher energy levels than the solid motors of equivalent size, 3) fuel grain robustness (no catastrophic failures due to fuel grain cracks), 4) low cost (there are no pumps necessary, thus the engine has the simplicity of a solid rocket), and 5) safety.[9] The hybrid motors are not categorized as highly explosive because the oxidizer is separate from the fuel. This is not true for the solid rocket motors. The safety feature of the hybrid motors also adds to their cost-effectiveness. With the development of new oxidizers and fuels, the hybrid rocket motors are improving in efficiency and could be a viable replacement for both solid and liquid fueled systems, with the added benefit of cost savings. This technology has direct application to tactical missiles.

Guidance Law Development

To utilize LQG optimal control theory, the missile math model must be linear and the cost functional must be quadratic in form. The linear math model selected is

$$\dot{\bar{X}} = A\bar{X} + Bu \tag{1}$$

where $\bar{X}$ is the state vector made up of the three components of target-to-missile position, target-to-missile velocity, and target acceleration, all relative to some fixed inertial reference frame, i.e.,

$$\bar{X} = \begin{bmatrix} \bar{S}_R \\ \bar{V}_R \\ \bar{A}_T \end{bmatrix} \tag{2}$$

and

$$\dot{\bar{X}} = \begin{bmatrix} \bar{V}_R \\ \bar{A}_T - \bar{A}_M \\ -\lambda_T \bar{A}_T \end{bmatrix} \tag{3}$$

This gives the following A and B matrices:

$$A = \begin{bmatrix} 0 & I & 0 \\ 0 & 0 & I \\ 0 & 0 & -\lambda_T I \end{bmatrix}, \qquad B = \begin{bmatrix} 0 \\ -I \\ 0 \end{bmatrix} \tag{4}$$

Note that the target acceleration is modeled as a first-order Markov process where λ_T is the target acceleration response time coefficient.

The cost functional to be minimized is

$$J = \frac{1}{2}\bar{X}^T(t_f)S_f\bar{X}(t_f) + \frac{1}{2}\int_{t_0}^{t_f} \bar{u}^T R\bar{u}\,\mathrm{d}t \tag{5}$$

where S_f and R are the weighting factors for final target-to-missile position and the control over the entire flight, respectively. The resultant control solution is

$$A_{M_X} = G_{c_x}\left[\left(S_{R_X}/t_{go}^2\right) + \left(V_{R_X}/t_{go}\right) + K_T A_{T_X}\right] \tag{6}$$

$$A_{M_Y} = G_{c_y}\left[\left(S_{R_Y}/t_{go}^2\right) + \left(V_{R_Y}/t_{go}\right) + K_T A_{T_Y}\right] \tag{7}$$

$$A_{M_Z} = G_{c_z}\left[\left(S_{R_Z}/t_{go}^2\right) + \left(V_{R_Z}/t_{go}\right) + K_T A_{T_Z}\right] \tag{8}$$

where the elements appearing in the guidance law equations are described as follows:

$S_{R_x}, S_{R_y}, S_{R_z}$ = three components of relative position vector $\bar{S}_R$ referenced to the missile body
$V_{R_x}, V_{R_y}, V_{R_z}$ = three components of relative velocity vector $\bar{V}_R$ referenced to the missile body
$A_{M_x}, A_{M_y}, A_{M_z}$ = three components of missile acceleration command vector $\bar{A}_M$ referenced to the missile body
$G_{c_x}, G_{c_y}, G_{c_z}$ = navigational gain (usually set to 3)
K_T = target acceleration gain, where

$$K_T = \frac{e^{-\lambda_T t_{go}} - \lambda_T t_{go} + I}{\lambda_T^2 t_{go}^2} \tag{9}$$

and t_{go} is the time-to-go,[4]

$$t_{go} = \frac{2S_{RX}}{-V_{RX} + \sqrt{V_{RX}^2 + 4S_{RX}A_{XX}/3}} \tag{10}$$

where A_{XX} is the difference between the missile acceleration command and K_T times the target acceleration in the axial direction, i.e.,

$$A_{XX} = A_{M_X} - K_T' A_{T_X} \tag{11}$$

where K_T' is K_T evaluated at the previous time interval.

The time-to-go algorithm has the advantage of explicitly accounting for the missile's axial acceleration, which has been ignored in the past, thus resulting in more optimal lateral and normal acceleration commands. Note that A_{M_X} in Eq. (6) is the command acceleration to the missile's thrust and is not used in a missile with a solid rocket motor.

Adapting Guidance Law for Hybrid Rocket Motor Thrusting

The guidance law from Eqs. (6–8) lends itself quite easily to providing the thrust control to the hybrid rocket motors. For a missile with a solid rocket motor, only Eqs. (7) and (8) are used to command missile accelerations. For the missile with a hybrid rocket motor, Eq. (6) can be used to provide thrust control. In a high off-boresight launch, the missile must have high lateral maneuverability. In these situations, the missile's rocket engines must reduce thrust until the off-boresight angle (OBA) is reduced to a small value and then increase their thrust. To aid the guidance law, the following axial navigational gain, G_{c_x}, was selected:

If OBA > 40 deg,

$$G_{c_x} = 2.7 \tag{12}$$

If OBA < 40 deg,

$$G_{c_x} = 3.6 \tag{13}$$

This further reduces the thrust command at high OBAs and increases the thrust command at low OBAs. These gains were chosen from a statistical evaluation of simulated missile performance in a wide variety of high off-boresight launch conditions. They do not necessarily represent the optimal choice. An assumption is made that any OBA greater than 40 deg was considered high.

Proportional Navigation Guidance Law

Proportional navigation (PRO-NAV) is the most commonly used guidance scheme for tactical air-to-air missiles for over 40 years.[3] There are several reasons for this. First, PRO-NAV is very effective in guiding missiles that are launched under restricted launch conditions (near collision course) and that are intercepting low-maneuverability-type aircraft. Second, PRO-NAV is relatively easy to implement. The PRO-NAV guidance law is

$$A_{M_X} = 0 \tag{14}$$

$$A_{M_Y} = -G_{C_Y}\dot{R}\dot{\sigma}_r \tag{15}$$

$$A_{M_Z} = G_{C_Z}\dot{R}\dot{\sigma}_q \tag{16}$$

where G_{c_y} and G_{c_z} are the navigational gain (usually both are set to 3 or 4 for PRO-NAV), $\dot{R}$ is range rate, and $\dot{\sigma_r}$ and $\dot{\sigma_q}$ are the line-of-sight rate in yaw and pitch, respectively.

The limitations of PRO-NAV can be seen when it is derived from optimal control theory. PRO-NAV is optimal given the following assumptions[3]: 1) The target has zero acceleration in both magnitude and direction, 2) the missile has instantaneous response and complete control over the total missile acceleration vector, 3) the line-of-sight angle (the angle between the target and the direction the missile is pointed) is small over the entire engagement, and 4) the missile has a velocity advantage over the target and the rate of change of the distance between the missile and the target is constant. Assumption 3 says that the missile has to be pointed nearly directly at the target, on a collision course. The combination of this with assumptions 1 and 4 means that the acceleration along the line of sight due to the missile must be zero.

The net result of this is that you only have lateral control (pitch and yaw) of the missile and no control over the axial direction of the missile, as seen in Eqs. (14–16). This is reasonable for a missile with a solid rocket motor because axial acceleration control is not needed. However, PRO-NAV cannot be used to provide throttle commands to the hybrid rocket motor.

Extended Kalman Filter

The EKF used to estimate the target-to-missile position, velocity, and target acceleration is described as follows.[3]

State model:

$$\dot{X} = AX(t) + Bu(t) + \omega(t), \qquad \omega(t) \approx N[0, Q(t)] \quad (17)$$

$$X(0) \approx N(X_0, P_0) \quad (18)$$

Measurement model:

$$Z_k = g[X(t_k)] + \upsilon_k, \qquad \upsilon_k \approx N(0, R_k) \qquad k = 1, 2, 3, \ldots \quad (19)$$

where

$X(t)$	= EKF states (missile-to-target position, velocity, and target acceleration)
A	= state matrix
$Bu(t)$	= state forcing function
$\omega(t)$	= zero mean, white sequence of covariance $Q(t)$
$Q(t)$	= systems' dynamics modeling error matrix
Z_k	= EKF measurements
υ_k	= zero mean, white sequence of covariance R_k
R_k	= measurement error matrix
X_0	= initial value of states
P_0	= initial value of covariance of states

and g is described by

$$g[X(t_k)] = \begin{bmatrix} A_Z \\ E_l \end{bmatrix} \quad (20)$$

where

$$Az = \tan^{-1}(R_Y/R_X) \quad (21)$$

$$El = \tan^{-1}\left(\frac{R_Z}{\sqrt{R_X^2 + R_Y^2}}\right) \quad (22)$$

Figure 1 shows the relationship of the azimuth and elevation angles to the filter's states where R_x, R_y, and R_z are the x, y, and z components of the range-to-target vector.

The propagation equations of the state estimates ($\hat{X}$) and error covariance ($\hat{P}$) are

$$\bar{X}(t_k) = \Phi(t_k, t_{k-1})\hat{X}(t_{k-1}) + \int_{t_{k-1}}^{t_k} \Phi(t_k, \tau)Bu(\tau)\,\mathrm{d}\tau \quad (23)$$

$$\bar{P}(t_k) = \Phi(t_k, t_{k-1})\hat{P}(t_{k-1})\Phi^T(t_k, t_{k-1}) + Q_k \quad (24)$$

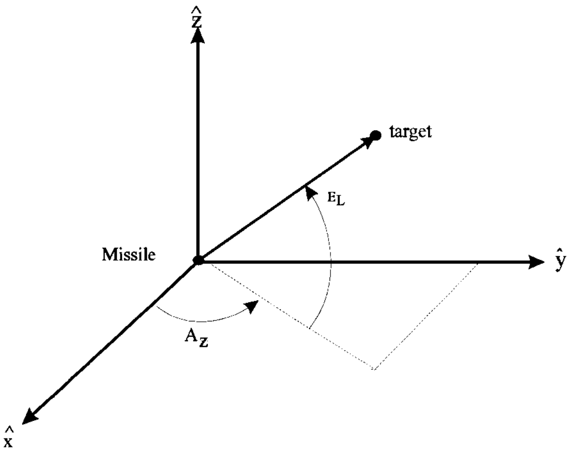

Fig. 1 Angular measurements for the EKF.

where $\bar{X}(t_k)$ is the propagated state estimate, $\bar{P}(t_k)$ is the propagated error covariance estimate, and Φ is the state transition matrix.

The update equations for the filter states and covariance matrix are

$$\hat{X}(t_k) = \bar{X}(t_k) + K(t_k)\{Z(t_k) - g[\bar{X}(t_k)]\} \quad (25)$$

$$\hat{P}(t_k) = \{I - K(t_k)H[\bar{X}(t_k)]\}\bar{P}(t_k) \quad (26)$$

where K is the Kalman gain matrix described by

$$K(t_k) = \bar{P}(t_k)H^T[\bar{X}(t_k)]\{H[\bar{X}(t_k)]\bar{P}(t_k)H^T[\bar{X}(t_k)] + R(t_k)\}^{-1} \quad (27)$$

and

$$H[\bar{X}(t_k)] = \left.\frac{\partial g[X(t_k)]}{\partial X(t_k)}\right|_{X=\bar{X}} \quad (28)$$

Performance Evaluation

The three guidance laws coupled with an EKF were evaluated using a three-degree-of-freedom simulation of the dynamics of an air-to-air missile vs a maneuvering target. The first guidance scheme involved using Eqs. (6–8) coupled with a traditional solid rocket motor. This motor generated a missile acceleration of 255 m/s^2 for 2.6 s, typical of a short-range air-to-air missile. This guidance law, EKF, and solid rocket motor combination will be referred to as AG1. The second guidance scheme used the same guidance algorithm equations coupled with a throttleable hybrid rocket motor. The guidance law is different in that Eq. (6) is used with the axial navigational gains in Eqs. (12) and (13) to command the thrust of the hybrid rocket motor. This guidance/EKF/motor scheme will be referred to as AG2. The motor was limited to a maximum acceleration of 255 m/s^2 and a total burn pulse of 255 × 2.6 N-s. This had the effect of limiting both guidance systems to the same amount of fuel and maximum thrust. For the first 0.4 s the missile was at maximum axial acceleration, 255 m/s^2, to clear the launch aircraft.

The third guidance law is proportional navigation [Eqs. (14–16)] coupled with the same solid rocket motor concept used by AG1. The extended Kalman filter was used to provide estimates of range rate $\dot{R}$ and the two line-of-sight rates $\dot{\sigma_r}$ and $\dot{\sigma_q}$. Navigational gains of 3 and 4 were used for PRO-NAV during the evaluation.

The simulation was designed to be fairly realistic. For all three guidance schemes, the missile was not allowed to maneuver laterally for the first 0.4 s, again to allow the missile to clear the launch aircraft. In addition, the missile was limited to a maximum lateral acceleration of 30 g (typical for a Sidewinder-type missile.) To simulate drag, the following drag model was used when the missile was not thrusting:

$$\bar{a}_D = -\tfrac{1}{2}\rho(1/\mathrm{BC})V_{\mathrm{rel}}^2(\bar{V}_{\mathrm{rel}}/V_{\mathrm{rel}}) \quad (29)$$

where

$\bar{a}_D$ = acceleration due to drag
ρ = atmospheric density
V_{rel} = velocity of the missile with respect to the atmosphere
BC = ballistic coefficient defined by

$$\text{BC} = M/C_D A \tag{30}$$

where

M = mass of the missile
C_D = coefficient of drag
A = cross-sectional area of the missile.

For this simulation, the ballistic coefficient was selected to be typical of a Sidewinder-type missile. The term M was selected as 87 kg, C_D was selected as 0.75, and A was selected for a missile with a diameter of 127 mm. The target used in this simulation incorporated a 9-g out-of-plane evasive maneuver. This missile/target combination was selected because it represents desired performance capabilities for the future guided weapons.

The input variables for the EKF were chosen for the air-to-air engagement.[3] The statistical matrices Q_k and R_k are

$$Q_k = \begin{bmatrix} 0 & 0 & 0 \\ 0 & Q_M I & 0 \\ 0 & 0 & Q_T I \end{bmatrix} \tag{31}$$

$$R_k = \begin{bmatrix} (0.25/R^2) + 5.625 \times 10^{-7} & \\ & (0.25/R^2) + 5.625 \times 10^{-7} \end{bmatrix} \tag{32}$$

where Q_M and Q_T were chosen as 14 m^2/s^2 and 3716 m^2/s^4, respectively. These two equations come from models used in Air Force laboratory basic research.[3]

For all three guidance schemes, an inner launch boundary and an outer launch boundary were generated for numerous simulated flyouts. The inner launch boundary defines the minimum range from which the missile can be launched and achieve a hit. [A hit is scored any time the point of closest approach (miss distance) is within 3 m of the target.] The outer launch boundary defines the maximum range from which the missile can be launched and achieve a hit. The two boundaries combined represent the launch envelope for the missile. A set of launch conditions was selected to provide a good sampling of the weapon's performance under high off-boresight launch conditions.[1,2]

1) The missile and the target are at the same speed and flying straight and level at launch (0.87 Mach).

2) The missile and the target are at the same altitude at launch (4675 m).

3) The initial aspect angle (the angle between the missile's velocity vector and the target's velocity vector) is 180 deg.

4) The initial OBA is varied from 40 to 80 deg.

These launch conditions have been identified by the United States as a good test for high off-boresight, air-to-air engagements, with the exception that condition 4 was limited to 60 deg. This effort expands the launch conditions to include a large range of OBAs. The geometry is depicted in Fig. 2.

The target travels straight until the missile is within 2000 m; then the target pulls a 9-g evasive out-of-plane maneuver. A comparison of the inner launch boundaries and the outer launch boundaries for AG1, AG2, and PRO-NAV are shown in Tables 1 and 2. Note that the results are shown for the guidance laws using perfect state information and the more realistic situation where the guidance laws are using state estimates from the EKF.

So that engineers can better understand what is happening, plots of the missile/target engagement are generated for AG1 and AG2 at the launch conditions of 60-deg OBA and initial launch range of 4000 and 4200 m. These can be seen in Figs. 3–10. The x–y axes come from Fig. 2 and the z axis is vertical. In addition, the axial acceleration profiles (at the 4000-m launch range) for the hybrid rocket motor and the solid rocket motor are shown in Figs. 11 and 12. The plots in Figs. 3–12 are based on the assumption that the missile-to-target state information is known perfectly.

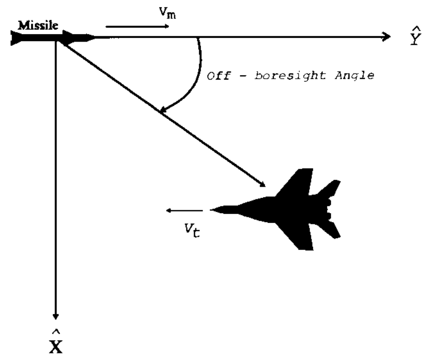

Fig. 2 Initial missile/target engagement geometry.

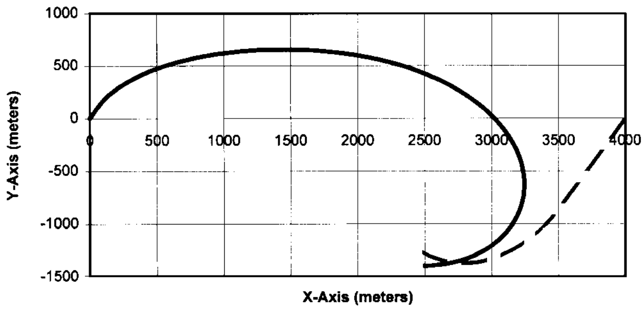

Fig. 3 AG1: x–y axis for 4000-m, 60-deg OBA launch; ——, missile, and - - -, tar get.

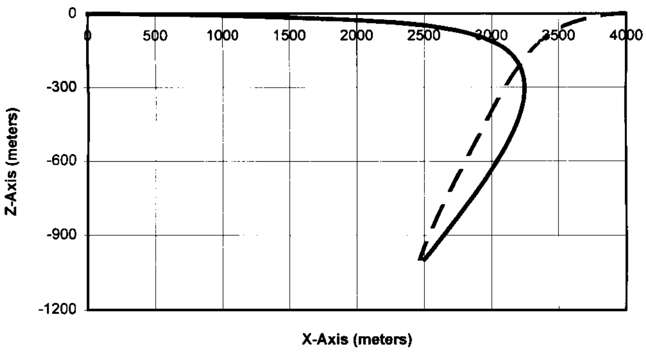

Fig. 4 AG1: x–z axis for 4000-m, 60-deg launch; ——, missile, and - - -, target.

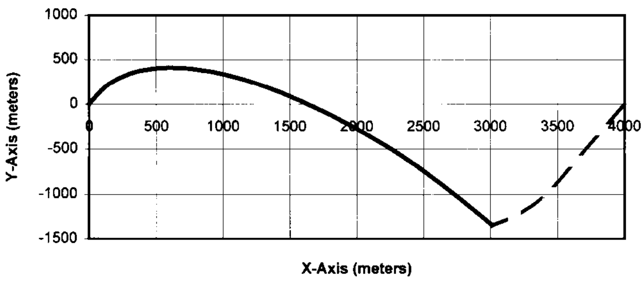

Fig. 5 AG2: x–y axis for 4000-m, 60-deg OBA launch; ——, missile, and - - -, tar get.

Results

Tables 1 and 2 show that the AG2 guided missile provides a significant improvement in high-OBA, air-to-air engagements over the AG1 guided missile. In particular, the largest improvements come from the close-in engagements, where AG2 has a much smaller inner launch boundary than AG1. For the more realistic situation where the guidance laws use the state estimates from the EKF, the improvements in the inner launch boundary due to AG2 range from

Table 1 Inner launch boundaries

	Minimum launch range, m							
	AG1 solid rocket motor		AG2 hybrid rocket motor		PRO-NAV gain = 3.0		PRO-NAV gain = 4.0	
OBA, deg	Perfect states	EKF states	Perfect states	EKF states	Perfect states	EKF states	Perfect states	EKF states
40	3800	3900	3700	3700	4300	——	3900	3900
50	4400	4400	3600	3600	4700	——	4500	4800
60	4200	4400	3200	3200	5100	——	4600	——
70	3700	4000	2300	2700	——	——	——	——
80	——	——	2100	2200	——	——	——	——

Table 2 Outer launch boundaries

	Maximum launch range, m							
	AG1 solid rocket motor		AG2 hybrid rocket motor		PRO-NAV gain = 3.0		PRO-NAV gain = 4.0	
OBA, deg	Perfect states	EKF states	Perfect states	EKF states	Perfect states	EKF states	Perfect states	EKF states
40	6700	6000	6700	6500	6500	——	6600	5900
50	6400	5600	6500	6100	6400	——	6400	5800
60	6000	5200	6400	6000	5900	——	6100	——
70	5300	4200	5700	5400	——	——	——	——
80	——	——	4900	4800	——	——	——	——

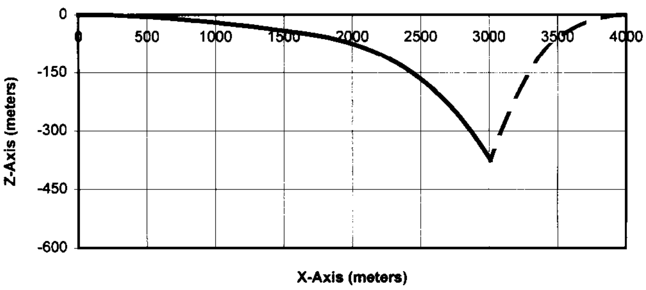

Fig. 6 AG2: x–z axis for 4000-m, 60-deg launch; ——, missile, and - - -, target.

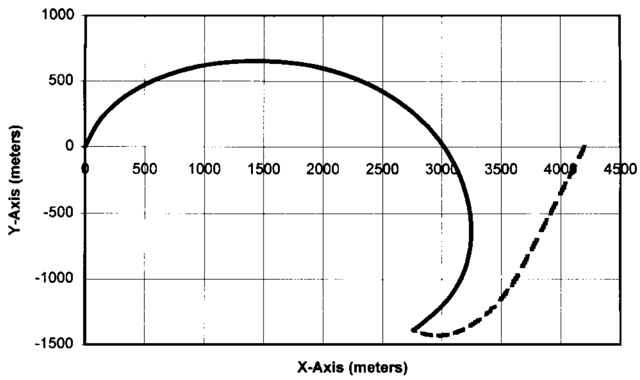

Fig. 7 AG1: x–y axis for 4200-m, 60-deg OBA launch; ——, missile, and - - -, tar get.

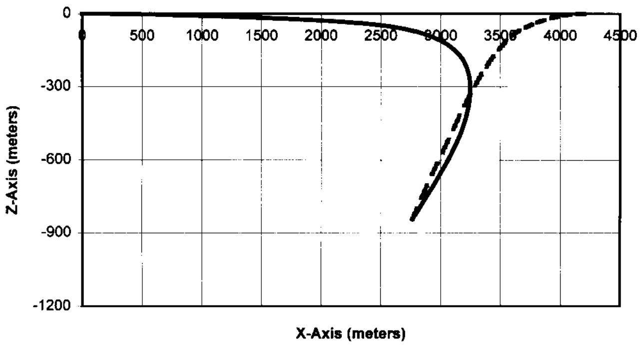

Fig. 8 AG1: x–z axis for 4200-m, 60-deg launch; ——, missile, and - - -, target.

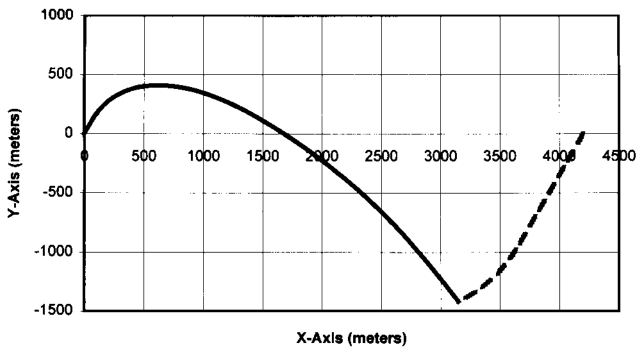

Fig. 9 AG2: x–y axis for 4200-m, 60-deg OBA launch; ——, missile, and - - -, tar get.

5% at 40-deg OBA to 32% at 70-deg OBA. The improvements in the maximum launch ranges using AG2 were almost as impressive. The outer launch boundary was increased by 8% at 40-deg OBA to 28% at 70-deg OBA. Note that AG2 was effective for up to 80-deg OBA, whereas AG1 was effective to 70-deg OBA.

The results of the 4000- and 4200-m, 60-deg OBA launch provide a good understanding of the benefits of AG2. The first launch condition was at 4000 m. With the AG1 guided missile pulling maximum axial acceleration for the first 2.6 s after launch (Fig. 11), it is dynamically incapable of turning fast enough to catch up with the target, shown in Fig. 3. The AG2 guided missile is able to reduce axial acceleration after the first 0.4 s, maneuver laterally, and resume axial acceleration to pursue the target (Fig. 12). Figure 5 shows the AG2 guided missile pulling a much tighter turn than the AG1 guided missile in Fig. 3, thus pointing toward the target quicker. For the 4200-m launch condition, both the AG1 and AG2 guided missiles were able to intercept the target. The difference here is in how long each of them took to reach the target. The AG1 guided missile took 8.31 s, whereas the AG2 guided missile took 6.41 s, a 23% reduction in time of flight. This is apparent from the tighter turn the AG2 guided missile took (Fig. 9) over the AG1 guided missile (Fig. 7).

Proportional navigation with a navigational gain of 3 was totally ineffective when used with an EKF. When the navigational gain was increased to 4, PRO-NAV was somewhat effective at 40 and 50-deg OBA, but it still was not as good as AG1 or AG2.

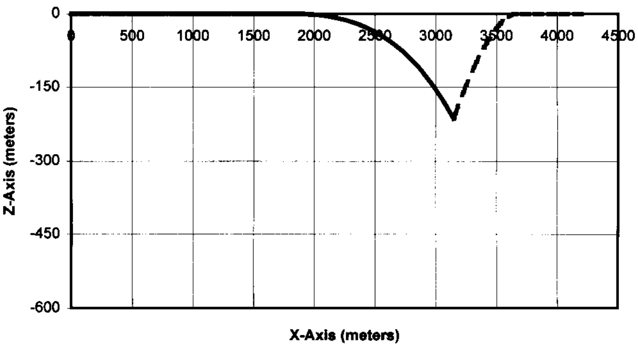

Fig. 10 AG2: x–z axis for 4200-m, 60-deg launch; ——, missile, and - - -, target.

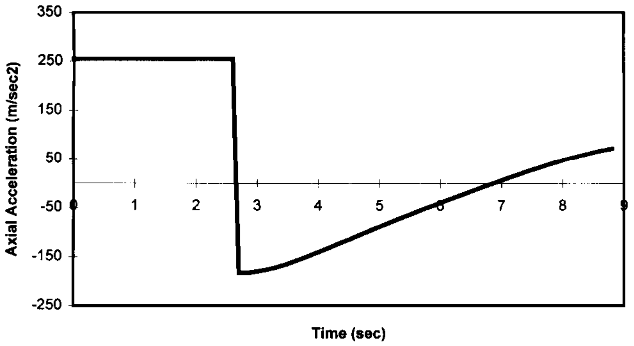

Fig. 11 Axial acceleration profile for missile with solid rocket motor.

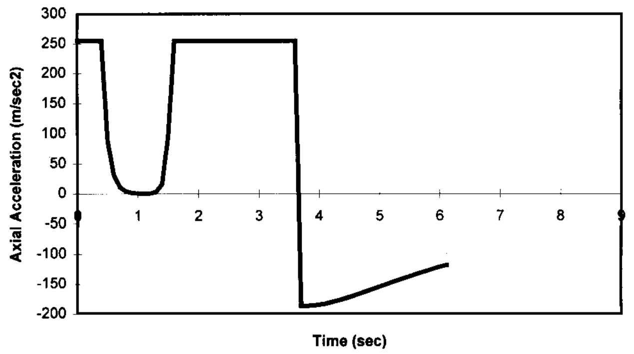

Fig. 12 Axial acceleration profile for missile with hybrid rocket motor.

Conclusions

The results show that current air-to-air missiles with a passive seeker will be ineffective using traditional proportional navigation guidance and a solid rocket motor against highly maneuverable targets in a high off-boresight launch condition. More advanced guidance schemes like the LQG guidance laws shown in this paper, coupled with an EKF, offer significant missile performance under these launch conditions. Furthermore, an advanced guidance law with a hybrid rocket motor can provide significant missile performance improvements over a similar guidance law with a solid rocket. This is especially true for close-in engagements. With a hybrid motor, the advanced guidance law is able to control the axial acceleration of the missile and provide a more optimal performance.

When the EKF was used to provide estimates for the advanced guidance law, there were no significant losses in performance. The bottom line is that the performance of an air-to-air tactical missile with a passive seeker can be greatly improved when a combination of a hybrid rocket motor, an advanced guidance law, and EKF is used.

In addition to AG2 improving the inner and outer launch boundaries over AG1, AG2 decreases the missile's time of flight to target over AG1 for all launch conditions. For the 4200-m, 60-deg OBA launch case (where the missile hits the target with both AG1 and AG2), the time of flight of the missile was reduced by 23% using AG2. On average, the AG2 guided missile's time of flight was reduced by 5% for close-in engagements with 40–50 deg launch OBAs and 21% for close-in engagements with the higher 60–70 deg launch OBAs. This is significant because it reduces the time the target aircraft has to respond. This provides an increased survivability of the friendly forces.

Finally, the AG2 guidance scheme provides the additional advantage of cost savings in that it can be adapted to fit the current inventory of short-range air-to-air missiles. Specifically, for the class of Sidewinder missiles, the solid rocket motor could be replaced with a hybrid rocket motor and advanced guidance package. This does not eliminate the need for continued research in advanced missile airframes, thrust vectoring, etc. It provides a cost-effective means of upgrading current missile technology.

References

[1]Dornheim, M. A., and Hughes, D., "U.S. Intensifies Efforts to Meet Missile Threat," *Aviation Week and Space Technology*, Oct. 1995, pp. 36–39.

[2]Dornheim, M. A., and Hughes, D., "Cheaper Missile Changes Pushed," *Aviation Week and Space Technology*, Oct. 1995, p. 42.

[3]Riggs, T. L., and Vergez, P. L., "Advanced Air-to-Air Missile Guidance Using Optimal Control and Estimation," U.S. Air Force Armament Lab., AFATL-TR-81-56, Eglin AFB, FL, June 1981.

[4]McClendon, J. R., and Vergez, P. L., "Applications of Modern Control and Estimation Theory to the Guidance of Tactical Air-to-Air Missiles," *Proceedings of the Second Meeting of the Coordinating Group on Modern Control Theory*, Aberdeen Proving Grounds, MD, 1980.

[5]Riggs, T. L., "Optimal Control and Estimation for Terminal Guidance of Tactical Missiles," *Proceedings of AGARD—292*, 1980, pp. 23-1–23-11.

[6]Vergez, P. L., "Linear Optimal Guidance for an AIM-9L Missile," *Journal of Guidance and Control*, Vol. 4, No. 6, 1981, pp. 662, 663.

[7]Vergez, P. L., "High Off-Boresight Guidance for Tactical Missiles," *Journal of Optimal Control Applications and Methods* (submitted for publication).

[8]Sellers, J. L., *Understanding Space, An Introduction to Astronautics*, McGraw–Hill, New York, 1994, pp. 490–497.

[9]Humble, R. W., Henry, G. N., and Larson, W. J., "Space Propulsion Analysis and Design," *Space Technology Series*, McGraw–Hill, New York, 1995, pp. 365–439.